UC Riverside
UC Riverside Electronic Theses and Dissertations

Title

Antimicrobial Behavior of Novel Surfaces Generated by Electrophoretic Deposition and Breakdown Anodization

Permalink

https://escholarship.org/uc/item/7vn9s8jq

Author

Flores, Jessamine Quijano

Publication Date

2013

Peer reviewed|Thesis/dissertation

UNIVERSITY OF CALIFORNIA
RIVERSIDE

Antimicrobial Behavior of Novel Surfaces Generated by Electrophoretic Deposition and
Breakdown Anodization

A Thesis submitted in partial satisfaction
of the requirements for the degree of

Master of Science

in

Microbiology

by

Jessamine Quijano Flores

December 2013

Thesis Committee:
        Dr. Sharon Walker, Chairperson
        Dr. Marylynn Yates
        Dr. David Jassby

The Thesis of Jessamine Quijano Flores is approved:

_____

_____

_____

Committee Chairperson

University of California, Riverside

Acknowledgments

This accomplishment has been made possible by my amazing advisor Dr. Sharon Walker. I would like to thank her for her continual support in both professional and personal matters. Dr. Walker is an ideal advisor to have; she has devoted time to mold me into becoming a critical thinker and kept me motivated throughout this project. I would also like to thank my thesis for masters' committee members Dr. Marylynn Yates and Dr. David Jassby for their time and appreciated comments.

This research was in collaboration with the Department of Mechanical Engineering from the Massachusetts Institute of Technology. Dr. Culle Buie and Young Soo Joung contributed to this research with engineering surfaces used in the study and also with significantly surface analysis.

My research advanced because of the amazing research members and alumni in our research group. Alicia Taylor was a continual support during this project with helpful insights in many areas. Dr. Nichola Kinsinger was an enormous help in analyzing data and aiding me in composing this thesis. I would also like to thank Dr. Ian Marcus for inspiring me to join Dr. Walker's lab by showing me the amazing projects that were being conducted during my rotation and for aiding me in statistical analysis among other things. I would also like to thank Risa Guysi, Ryan Honda and Jacob Lanphere for their continual support and assistance in laboratory procedures.

My sincere appreciation goes to Dr. Richard Cardullo for being supportive and an amazing coordinator for my Fellowship Bridge to the Doctorate that was supported by the National Science Foundation (NSF).

Dedication

I dedicate this to my family and friends whom have supported me in this incredible journey. This achievement could not have been made without my parents struggle to give their children a fighting chance in succeeding in life by relocating to the United States. My parent's prayers without a doubt have allowed me to reach this amount of accomplishment and I thank them sincerely for this. My husband Ruben has been a pillar in holding me up in times of hardship, which has allowed me to triumph. My friends Diana Villa and Cynthia Guevara were of great emotional support in my educational journey.

ABSTRACT OF THE THESIS

Antimicrobial Behavior of Novel Surfaces Generated by Electrophoretic Deposition and
Breakdown Anodization

by

Jessamine Quijano Flores

Master of Science, Graduate Program Microbiology
University of California, Riverside, December 2013
Sharon L. Walker, Chairperson

Managing biofouling is a critical aspect in a wide range of industries and
addressing this concern is of optimal interest. In this study, the mass transfer of a model
marine bacterium (*Halomonas pacfica g*) was investigated on engineered surfaces
ranging from superhydrophobic to superhydrophilic. The quantification of the deposition
kinetics was achieved using a specially designed parallel plate flow chamber system
under a range of relevant solution chemistries on the test sufaces. *Halomonas pacifica g*
was further characterized to determine its zeta potential and hydrophobicity. Test surfaces
were generated via breakdown anodization or electrophoretic deposition, and properties
including surface roughness, contact angle, and capillary diffusivity were quantified. The
greatest deposition was observed on of the superhydrophilic surface, which had micro-
and nano- scale hierarchical structures composed of titanium oxide on a titanium plate.
Conversely, one of the hydrophobic surfaces with micro-porous films overlaid with
polydimethylsiloxane appeared to be most resistant to cell attachment.

Table of Contents

List of Figures

List of Tables

1. **Introduction**

   Biofouling is problematic for a variety of industries including cosmetics,

pharmaceuticals, medical devices, and global marine industries [1-3] leading to

staggering costs. As of 2010, it was estimated that the annual cost due to hull fouling for

current U.S. Navy ships and infrastructure ranged from $180-250 million [4]. Those

costs are directly related to cleaning and coating costs, as well as frictional drag that

increases fuel consumption. The fouling process on marine surfaces begins with bacterial

colonization and biofilms, followed by other microorganisms such as unicellular algae

(i.e. diatoms) and eventually invertebrates such as soft corals, sponges, barnacles, and

mussels [5]. The approach to combat biofouling may differ by industry although the

underlying challenge is the same for all, which is in the inhibition of the initial stages of

bacterial attachment to prevent microbial biofilms [6].

   The ever-present battle to inhibit fouling on ships has been addressed as early as the

1500s, with the use of copper plates on wooden ship hulls to decrease fouling [2, 7]. By

the 1960's antifouling paints, which contain biocide materials such as copper and

tributyltin (TBT) became commonplace for the prevention of cell adherence due to the

leaching of these materials. However, it was discovered that the corrosion process of

copper lead to the release of cuprous oxide that interfere with cell division and that the

copper and TBT were toxic to marine organisms [8, 9]. This led to the International

Maritime Organization to ban TBT in 2001 due to its high toxicity and long half-life of 3

months [10]. Copper having lower toxicity level is currently under review by the US EPA

for future restrictions, with the final outcome of that review anticipated in 2015 [11, 12].

There are three principal approaches to combat biofouling: the first employs the direct use of biocides as shown prior, the second is mechanical detachment, and the third is surface modification to prevent cell adherence. Antibiotics and cleaning chemicals are other biocides that are used to kill and degrade biofilms [13]. The medical community has attempted to load antibiotics onto medical devices to prevent infections and a recent study demonstrated a novel coating that slowly released antibiotics as a potential strategy to prevent specific microbial adherence [14]. Cleaning chemicals are used to degrade biofilms in dental unit waterlines to prevent patients and staff from exposure to these microorganisms [15]. The second principal approach once again is mechanically detaching attached microorganisms, but it has been shown that mechanical detaching fouling from ship hull has high maintenance concerns compared to other methods [16].

The final principal approach has been accomplished by the efforts of the material science community to explore novel surface modification techniques in an effort to develop anti-microbial, non-toxic surfaces through chemical and or structural modification [17-24].   Examples of such treatments include coating with self-assembled monolayers (SAMs), which can have finely tuned chemical properties: wettability, controlled functional groups, or charge density [21, 23, 24]. SAMs with ω-substituted alkane thiolates on gold, have been reported to have a positive correlation with spore attachment with increased surface hydrophobicity [17]. Many chemical coatings which incorporate such effective functional groups within polymeric materials have been investigated such as siloxane urethane, poly(ethylene glycol) polymers and combinations of various materials such as patterned poly(ethylene glycol) and fluorinated surfaces [19].

2

The production of fluorinated polymers that create hydrophobic surfaces were also found to be effective in generating surfaces that cells could be released from with sufficient shear force (i.e., ship movement or rinsing) [20]. Furthermore, aminoproply terminated poly(dimethyl siloxane) (PDMS) macromers prepared by a single amine group anchoring the PDMS were fabricated and shown to reduce biofilm retention. This was attributed to the hydrophobic nature of these surfaces, and it is thought that these types of materials can be further improved for antimicrobial properties [22]. Previously, it was also reported that zeolite-coated aluminum alloy and stainless steel surfaces had less bacterial cell deposition as compared to uncoated, bare metal surfaces [18].

There are a broad range of factors that are reported in playing a role in cell attachment including wettability/hydrophobicity, surface chemistry, surface roughness and topography, surface elastic modulus and color [17, 20, 25-29]. Wettability has been shown to be of great importance in both field and laboratory assays and thus a factor that must be addressed when developing antifouling surfaces [17, 25]. Surface roughness and topography is indeed a feature that must be considered when engineering surfaces since it has been shown to alter attachment of bacteria [26, 27]. Elastic modulus of the surfaces have also been proven to be key in addressing bioadhesion and must be contemplated in selecting antifouling surfaces [28]. Color has been shown to have an impact on fouling behavior, higher densities of species were found to favor black colored surfaces rather than white in different surface materials [29-31].

This study was aimed to investigate the attachment of a model marine organism to novel surfaces created by a hybrid method of employing breakdown anodization (BDA)

[32] and electrophoretic deposition (EPD) [33] and to evaluate the surface treatments' ability to control cell adhesion. Upon obtaining the model surfaces, which ranged from superhydrophilic to superhydrophobic with different surface morphologies and surface hydrophobities, they were characterized in terms of hydrophobicity, surface roughness, and zeta-potential. This characterization was followed up with extensive experimentation to evaluate these surfaces' ability to minimize or maximize the quantification of bacterial mass transfer rates.

2. Material and Methods

2.1 Bacterial Cell Preparation

The model marine bacterium selected for this study, *Halomonas pacifica* (ATCC 27122), was previously obtained from the ATCC (American Type Culture Collection, Rockville, MD) due to its fouling properties [34]. This bacterium was labeled with enhanced green fluorescent protein (EGFP) and gentamicin resistance via electroporation for visualization and is referred to as *H. pacifica g* [35]. *H. pacifica g* is a non-motile rod-shaped gram-negative bacterium and is grown at 30 °C in artificial seawater composed of sea salts (38.5 g/L, Sigma-Aldrich, Buchs SG, Switzerland), bacteriological peptone (5 g/L, Sigma), and yeast extract (1 g/L, Sigma) with gentamycin sulfate antibiotic (30 mg/L, OmniPur, Gibbstown, NJ) [36]. Pre-cultures made from marine agar plates (55.1 g/L, BD Diagnostic Systems) were used to inoculate second cultures and grown for 16 hours for further deposition and characterization studies [37]. Harvesting of cells was done by centrifugation (accuSpin 3R centrifuge, Fisher Scientific, Pittsburgh,

PA) for 15 minutes at 3689 g and further rinsing the pelleted cells twice with 10 mM

KCl. The KCl solution was prepared with reagent-grade salt (laboratory grade, Fisher

Sci.) and deionized (DI) Water (Millipore, Billerica, MA) at an unadjusted pH (5.6-5.8).

2.2 Bacterial Surface Characterization

To analyze the relative hydrophobicity of *H. pacifica g* cells, a semi-quantitative

microbial adhesion to hydrocarbons (MATH) test was employed [38]. The relative

hydrophobicity of the organism in each of these solutions is reported at the percent of

total cells that partition into the model hydrocarbon (dodecane) [39]. Specifically, test

tubes were set up to have 4 mL of the cell suspension with 1 mL of n-dodecane

(laboratory grade, Fisher Sci.). Test tubes were vortexed (AutoTouch Mixer Model 231,

Fisher Sci.) for 2 minutes followed by a rest period of 15 minutes to allow phase

separation and the final absorbance reading after the rest period was compared to the

initial absorbance acquired after harvesting. The optical density of the cells in the

aqueous phase was measured using a spectrophotometer at 546 nm (BioSpec-mini,

Shimadzu Corp., Kyoto, Japan). A second solution condition (ionic strength (IS) =

100mM KCl) was also test to compliment conditions set up for deposition studies. *H.*

pacifica g cells were harvested and a suspension of cells was prepared to have an optical

density of 0.2-0.25 in 10 mM KCl at 546 nm. Ionic strengths of 10 mM and 100 mM

have been shown to correspond to freshwater and 5% seawater [40].

Determination of the zeta potential of the bacterial cells was conducted using a

ZetaPALS analyzer (Brookhaven Instruments Corp., Holtsville, NY) at 25 °C with

harvested cells suspended in 10 mM and 100 mM KCl solution. This test was repeated at least three times with freshly harvested cells and the measured electrophoretic mobility values were converted to zeta potential using the Smoluchowski equation [41].

2.3 Material Surface Preparations and Characterization

Quartz slides have previously been used to observe deposition behavior under electrostatically unfavorable [42] and favorable conditions [35] (when coated with positively charged amininosilane). In this study, unmodified quartz microscope slides (electron microscopy Diatome quartz microscope slide, 3"×1", Fisher Sci.) cut to fit (9×20 mm) within the flow chamber. Prior to the deposition experiments on to the quartz, samples were cleaned by submerging and sonicated in 2% Extran® solution (EMD chemicals Inc., Darmstadt, Germany) and for 15 minutes at room temperature, followed by a thorough rinse with deionized (DI) water. Next, the quartz samples were submerged in 2% RBS 35 detergent solution (Pierce Biotechnology, Rockford, IL) and sonicated for 15 minutes at 50 °C, followed by a DI water rinse. Finally, quartz samples were submerged in Nochromix (Godax Laboratories, Inc., Cabin John, MD) solution overnight and rinsed with DI water the following day and allowed to air dry prior to use in transport studies.

The novel surfaces tested were created by electrophoretic deposition (EPD) and breakdown anodization (BDA) to produce nano- and micro-porous surfaces [32, 33, 43, 44]. Figure 1 shows a schematic illustration of BDA and EPD methods used to develop varying surface structures. In the BDA method, titanium (Ti) plates (ultra-corrosion-

6

resistant titanium grade 2, 0.020" thick, McMaster, Santa Fe Springs, CA) were used as

anode and cathode electrodes that were submerged in an electrolyte solution (DI water,

pH = 3 adjusted using nitric acid, 70 % ACS reagent, Sigma-Aldrich). An electric

potential of 120 V was applied to the titanium electrodes for 30 min during the

anodization process. The solution temperature was maintained using circulating water
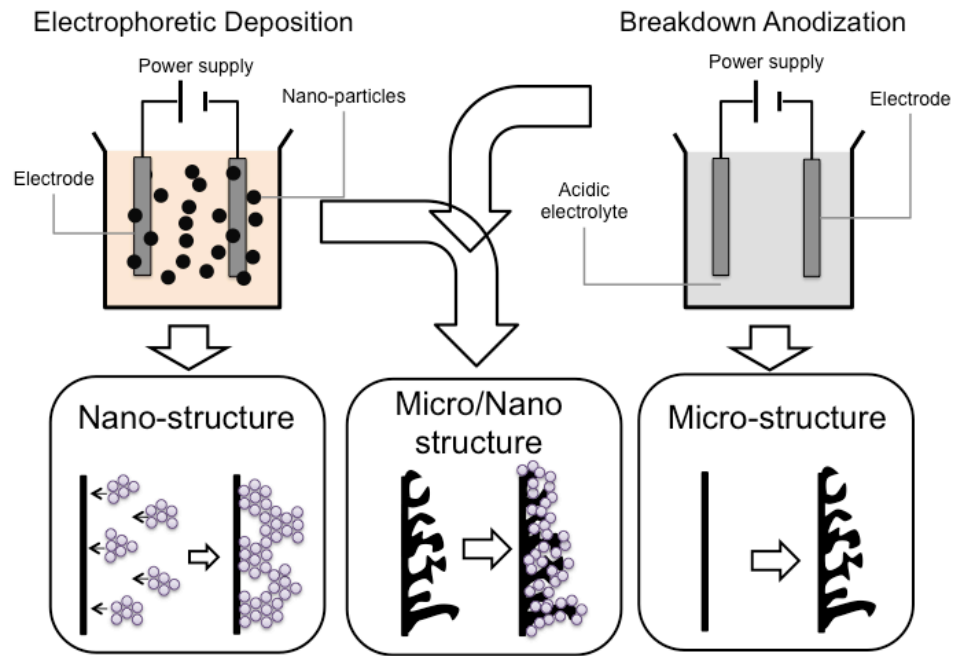
Figure 1. Fabrication processes for micro/nano hierarchically structured surfaces. For micro-porous structures, breakdown anodization (BDA) is used with different electrolyte temperatures. For nano porous structures, electrophoretic deposition (EPD) is used with different nanoparticles. The hierachical micro- and nano-porous structures are produced by a series of BDA and EPD. The electrolyte temperature and the nanoparticles affect the surface morpholgy and the surface energy, respectively.

(Polystate, Cole-Parmer, Vernon Hills, IL) surrounding the BDA cell since micro-

structures are strongly influenced by the temperature [32]. The resulting titanium dioxide

(TiO_2) surfaces generated by only BDA are referred to as TiO_2-B-10°C and TiO_2-B-25°C

(B signifies BDA, last digits signifies temperature in degree Celsius) unless otherwise

stated the materials were generated at a temperature of 24 °C.

7

EPD was used to produce nanostructure surfaces by depositing both hydrophobic silicon dioxide (SiO_2) nanoparticles coated with poly(dimethyl siloxane) (PDMS) and hydrophilic TiO_2 nanoparticles onto unmodified titanium plates. Noting that silicon dioxide (SiO_2) nanoparticles coated with (PDMS) will be refereed to just (P)SiO_2 for the remainder of this paper. (P)SiO_2 nanoparticles (14 nm, PlasmaChem, Berlin, Germany) were dispersed (1 g/L) in a mixture of 90 vol.% methanol (ACS Reagent, Baker analyzed) and 10 vol.% DI water. The resulting sample generated by EPD with (P)SiO_2 is referred to as (P)SiO_2-E (E indicates EPD). TiO_2 nanoparticles (20 nm, anatase, Sigma-Aldrich) were dispersed in acetic acid to achieve 1 g/L TiO_2 suspensions. An electric field of 30 or 60 V/cm was subjected to the electrodes for varying times, specifics found on Table 1. The suspension temperature was maintained constant at 24°C, to deposit nanoparticles onto the substrate.

For hierarchical micro- and nano-structured surfaces, BDA was conducted on titanium plates to make micro-porous layers followed by EPD of nanoparticles (either TiO_2 or (P)SiO_2) onto the micro-porous layers as described above. The resulting samples from the combination of BDA and EPD are referred to as TiO_2-BE, (P)SiO_2-BE-25°C, and (P)SiO_2-BE-75°C (BE indicates the combination BDA and EPA, last digits signifies temperature in degree Celsius). In EPD, temperature was maintained constant at 24°C.

The patterned BDA and EPD surfaces were further coated with PDMA such that specific levels of hydrophobicity and surface roughness could be generated. PDMS was coated on the surfaces by spin-coating at 3000 rpm for 1 min. The resulting samples are stated as PDMS-B or PDMS-E. These eight samples (TiO_2-B-10°C, TiO_2-B-25°C, TiO_2-

BE, (P)SiO$_2$-E, (P)SiO$_2$-BE-25°C, (P)SiO$_2$-BE-75°C, PDMS-B, and PDMS-E), which

have different morphologies and surface hydrophobicities, were positioned in the parallel

plate flow cell and utilized for the bacterial deposition experiments. Table 1 summarizes

the fabrication methods and materials used to produce the novel test surfaces with their

surface characteristics in terms of surface roughness (Ra), static contact angle, roll-off

angle, hydraulic diffusivity, and surface zeta-potential.

The morphology of the prepared surfaces was observed with a scanning electron

microscope (SEM, JEOL 6320FV Field-Emission High-resolution SEM and Zeiss, He-

Ion microscopy). Surface roughness was measured by a profilometer (tencor P-16 surface

profilometer (TM) Milpitas, CA) at five distinct points on each sample. The area scanned

was 2×4 cm^2 and the average root mean square (RMS) surface roughness was calculated

using commercial software provided by the profilometer manufacturer. Static contact

angles were measured by a goniometer (Kyowa, DM-CE1, Saitama, Japan). Averaged

contact angles were obtained from the measurements at four different points on each

sample. Static contact angles were calculated using the tangential curvefitting method.

From the advanding and receding contact angles, the roll-off angles were calculated [45].

The capillary rise measurement (CRM) has been used to characterize water transport

speed in terms of hydraulic diffusivity [46].

Name	Fabrication method	BDA condition (potential, time, electrolyte temperature)	Particles for EPD (material, size)	EPD condition (potential, time)	Spin coating (material, rotating-speed, time)
TiO$_2$-B-10°C	BDA	120 V, 30 min, 10 °C	N/A	N/A	N/A
TiO$_2$-B-25°C	BDA	120 V, 30 min, 25 °C	N/A	N/A	N/A
TiO$_2$-BE	BDA + EPD	120 V, 30 min, 10 °C	TiO$_2$, 20 nm	30 V, 2 min	N/A
(P)SiO$_2$-E	EPD	N/A	Hydrophobic SiO$_2$, 14 nm	60 V, 20 min	N/A
(P)SiO$_2$-BE-25°C	BDA + EPD	120 V, 30 min, 25 °C	Hydrophobic SiO$_2$, 14 nm	60 V, 10 min	N/A
(P)SiO$_2$-BE-75°C	BDA + EPD	120 V, 30 min, 75 °C	Hydrophobic SiO$_2$, 14 nm	60 V, 10 min	N/A
PDMS-B	BDA + PDMS	120 V, 30 min, 25 °C	N/A	N/A	PDMS, 3000 rpm, 1 min
PDMS-E	EPD + PDMS	N/A	TiO$_2$, 20 nm	30 V, 1.5 min	PDMS, 3000 rpm, 1 min

Table 1. Fabrication methods and conditions to produce different surface structures and energies. Breakdown anodization (BDA) and electrophoretic deposition (EPD) were used for micro and nano surface structures. Different electrolyte temperatures and different nanoparticles were used to change the surface structures and energies in BDA and EPD, respectively. To change surface energy, polydimethylsiloxane (PDMS) was spin-coated on the micro- and nano-structured surface

Surface zeta potential values were obtained using a clamping cell attached to a commercial streaming potential analyzer (Electro Kinetic Analyzer (EKA), Brookhaven Instruments, Holtsville, NY). The engineered samples were placed in the cell flat against a 10 mm pieced of grooved poly(methylmethacrylate) (PMMA) spacer, further described elsewhere [47]. Test solutions of 10 mM or 100 mM KCl were introduced into the rectangular channels of the PMMA spacer by the inlet/outlet tubing connected to Ag/AgCl electrodes. First, a sample coupon was loaded into the clamping cell and rinsed with DI water. Then, the zeta potential was characterized with DI water, 5 mM KCl, and 10 mM KCl as background solutions separately. All the measurements were performed at room temperature (23 °C) without adjusting pH.

2.4 Bacterial Deposition Studies

H. pacifica g deposition experiments employed a modified parallel plate flow chamber (PP) [48, 49] (product 31-010, GlycoTech, Rockville, MA) positioned on the stage of an upright fluorescent microscope (BX-52, Olympus). The inner dimension of the chamber are 6 cm×1 cm×0.0762 cm and is composed of a Plexiglas block that is mounted by a flexible silicon elastomer gasket and a microscope slide that vacuum grease seals all together. The flow deck has a groove (9 × 20 mm) where samples are held in place by vacuum grease. The fluid stream enters the chamber from a capillary tube that is connected to a syringe being pressed by a peristaltic pump at a flow rate of 0.1 mL/min, corresponding to an average flow velocity of 0.79 m/h, and a Péclet number of 6.47×10^{-4} [50]. The fluorescently labeled bacteria are imaged by a 40× long working

distance objective (UPlanFl, Olympus) using a filter at excitation and emission wavelengths of 480 nm and 510 nm, respectively (Chroma Technology Corp., Brattleboro, VT).

Deposition of *H. pacifica cells* was observed over a 30 minute period with images recorded with a digital camera (Demo Retiga EXI Monochrome, QImaging) every minute to determine the kinetics of deposition cells for each time interval. Enumeration of cells was determined by comparison of successive images. A suspension of cells (1×10^8 cells/mL) was utilized and the concentration was determined with a counting chamber (Bürker-Türk chamber, Marienfield Labora- tory Glassware, Lauda-Konigshofen, Germany). Deposition experiments were conducted at 10 and 100 mM KCl with unadjusted pH (5.6-5.8) at ambient temperature (22-25 °C). Engineered surfaces prepared by the techniques describe above were rinsed with DI water within the parallel plate flow cell prior to deposition experiments.

The number of bacterial cells deposited versus time was plotted and calculation of bacterial deposition flux (J) was achieved by dividing the initial slope of the line by the microscope viewing area (230 μm × 170 μm). The mass transfer rate coefficient for the bacteria, k_{pp}, is calculated using the bacterial deposition flux (J) and the bulk cell concentration, C_0, via [18, 41, 51]:

$$k_{pp} = \frac{J}{C_0} \tag{1}$$

Deposition experiments were conducted under chemically "unfavorable" conditions on quartz for the sake of comparison with the engineered surfaces. The mass transfer rate coefficients for these experiments are identified as k_{pp}.

3. Results & Discussion

3.1 Characterization *of H. pacifica g* cells

Analysis of the hydrophobicity (MATH test) data indicates 14.27±1.61% and

13.38±3.13% of *H. pacifica g* cells partition into the organic phase at 10mM and 100mM

KCl, respectively. This suggests that these bacterial cells are predominantly hydrophilic

at stationary growth phase as previously observed [34]. The bacterial cell zeta potentials

were -58.7±2.61 mV and -19.94±6.53mV at 10mM and100mM KCl, respectively. This

is also similar to what has been reported [18]. The zeta potential results indicate *H.*

pacifica g cells were negatively charged over the range of ionic strength conditions

tested, with the magnitude of the zeta potential decreasing with greater ionic strength.

3.2 Engineered Surface Characterization

Engineered surfaces were characterized for surface roughness, hydraulic diffusivity,

static contact angle, and roll-off angle, and zeta-potential as shown in Table 2. Micro and

nano-porous structures produced using the BDA, EPD, combined BDA with EPD, and

spin coating of PDMS on either BDA or EPD modified substrates are visible in SEM

images (Figure 2).

In the case of surfaces generated with the BDA technique (samples TiO_2-B-10°C

and TiO_2-B-25°C), the irregular micro-scale features which resulted in surface roughness

~20 μm (Figure 2a, Table 2) are attributed to the competing mechanisms of dissolution

and oxidation of the Ti plate during the anodization process without statistical

significance due to heterogeneity ($p > 0.05$). Interestingly, the micro-porous structures

produced by the use of BDA have sub-micron thin channels on the surfaces, which are observed in SEM images (Figure 2a).

At low electrolyte temperatures the oxidation reaction was observed to dominate resulting in an increased substrate mass where at higher electrolyte temperatures (> 50 °C) rapid dissolution was observed which facilitated micro-pore formation. All TiO_2 BDA surfaces showed nearly zero contact angles because of the titanium oxide, which is the surface material after BDA, and a very hydrophilic material with rough surface structures, but hydraulic diffusivity was found to have statistical difference between TiO_2-b-10°C and TiO_2-B-25°C from 86 ± 10.56 mm^2/s to 145 ± 3.42 mm^2/s ($p < 0.05$). Hydraulic diffusivity is an indicator of the speed at which the liquid can move along a surface. Because TiO_2-B-25°C has higher surface roughness, which is known as proportional to the effective pore radius, less viscous drag can be expected than TiO_2-B-10°C, resulting in faster water propagation.

In contrast to BDA, EPD-generated surfaces are observed to be more uniform due to the deposition of uniformly size nanoparticles with nanopores between the coagulated particles (Figures 2b and 2d). Roughness occurs on the nanoscale for EPD generated surfaces (rather than on the microscale). For example EPD roughness (sample (P)SiO$_2$-E) is 1 ± 0.09 μm significantly lower than the roughness produced using the BDA technique resulting in ~20 ± 10.17 μm roughness (samples TiO_2-b-10°C and TiO_2-B-25°C) [32].
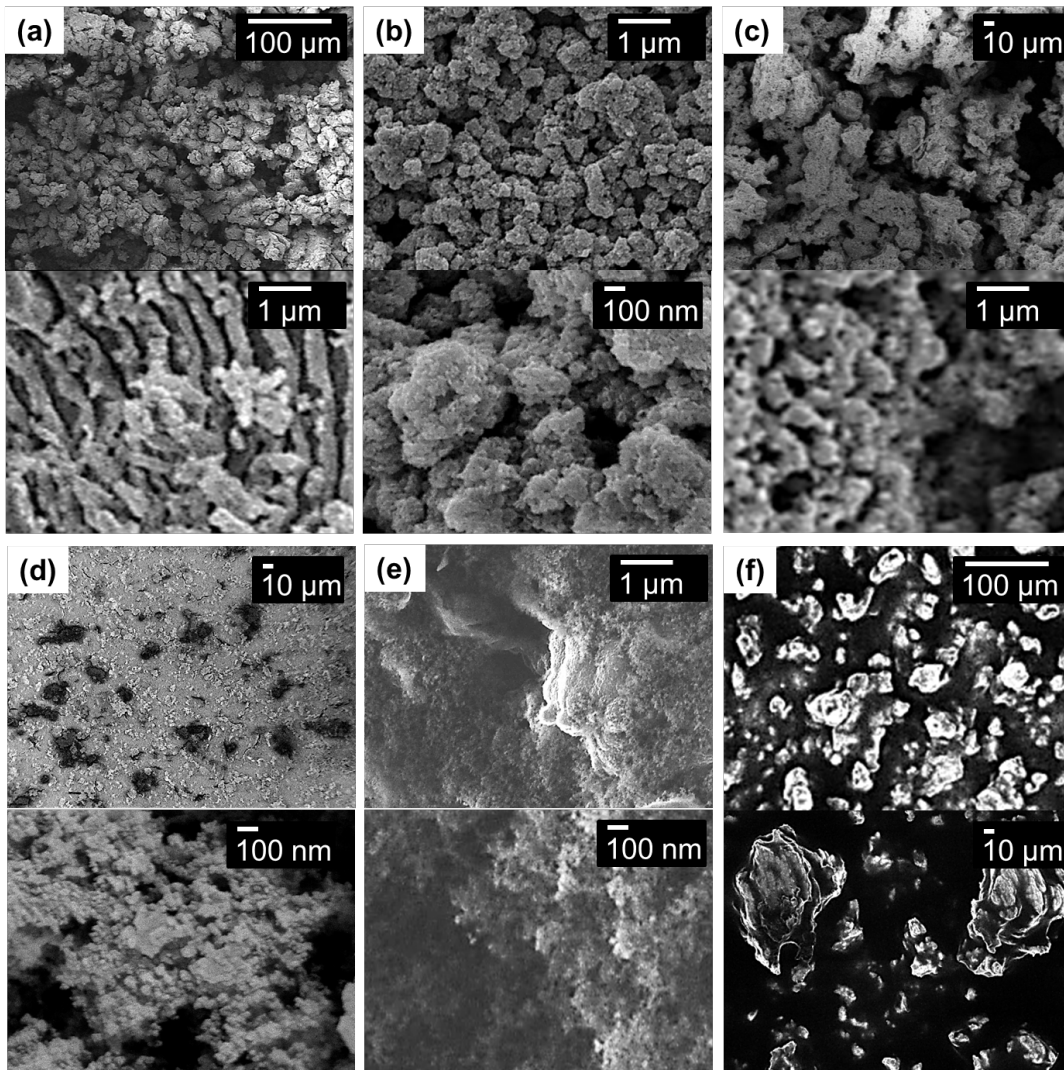
Figure 2. SEM images of the surfaces produced by the fabrication methods: breakdown anodization (BDA), electrophoretic deposition (EPD), and a spin coating with PDMS. The BDA surface consists of highly irregular entangled micro structures (a) while the surface deposited with TiO2 nanoparticles by EPD shows uniformly distributed nano-porous structures (b). Micro- and nano- porous structures are observed on the surface produced by the hybrid method of BDA and EPD (c). Deposits of hydrophobic SiO2 nanoparticles have nanoscale pores between agglomerated particles (d). The BDA surface coated with hydrophobic SiO2 nanoparticles show micro- and nano-porous structures (e). The BDA surface coated with PDMS by the spin-coating shows micro-bumps and PDMS coating layers between the structures (f). Surfaces (a)-(c) are superhydrophilic, surfaces (d)-(e) superhydrophobic, and surface (f) hydrophobic.

Name	Fabrication method	Surface roughness (mm)	Hydraulic diffusivity (mm^2/s)	Contact angle: q	Roll-off angle: q	Zeta Potential (mV)
Quartz	N/A	$(1.04\pm0.18)\times10^{-3}$	0	24±4.1	41±2.94	-20
TiO$_2$-B-10°C	BDA	18±8.62	86±10.56	0	N/A	-0.1±5.83
TiO$_2$-B-25°C	BDA	23±12.37	145±3.42	0	N/A	11.8±8.74
TiO$_2$-BE	BDA + EPD	15±3.69	60±3.68	0	N/A	34.5±3.62
SiO$_2$-E	EPD	1±0.09	N/A	159±2.64	2±0.80	9.0±3.34
SiO$_2$-BE-25°C	BDA + EPD	21±10.12	N/A	147±3.45	14±3.08	19.2±3.32
SiO$_2$-BE-75°C	BDA + EPD	9±1.33	N/A	141±4.39	5±1.69	10.4±5.91
PDMS-B	BDA + PDMS	11±4.45	N/A	110±4.34	5±2.33	4.85±1.69
PDMS-E	EPD + PDMS	3±1.90	N/A	107±3.07	> 90±4.78	-5.05±7.85

Table 2. The surface structures were characterized by a profilometer, and wetting properties were measured in terms of static contact angle, roll-off angle, and hydraulic diffusivity. Zeta potential was also measured at 10mM IS. Based on the contact angles, the prepared surfaces were classified as superhydrophobic (Samples TiO2-B-10°C, TiO2-B-25°C, TiO2-BE), superhydrophilic (Samples SiO2-E, SiO2-BE-25°C, SiO2-BE-75°C), and hydrophobic (Samples PDMS-B, PDMS-E)

When the method of BDA is followed by EPD for producing samples (TiO_2-BE, (P)SiO_2-BE-25°C and (P)SiO_2-BE-75°C), dual scales of micro- and nano-porous structures were successfully produced on the surfaces (Figures 2c and 2e) as illustrated in Figure 1 on how these methods produce such structures. Since the layer deposited by EPD are uniform and thin (see Figure 2c and 2e), the microporous structures were maintained after being coated with nanoparticles. By coating BDA substrates with TiO_2 nanoparticles via EPD (sample TiO_2-BE), the average surface roughness is slightly reduced by 3±10.82 μm in comparison to samples TiO_2-B-10°C and TiO_2-B-25°C; however, this was found to be insignificant due to heterogeneity of the surfaces ($p > 0.05$). BDA followed by EPD fabrication results in surfaces with wide ranges of surface roughness, hydrophobicity, and hydrophilicity (as shown in Table 2) dictated by dictated by the coating material (TiO_2, (P)SiO_2, or PDMS).

When BDA surface is coated with PDMS, microscale bumps are generated, resulting in PDMS being infused between the micro-structures (Figure 2f). Coating the BDA substrate with PDMS (sample PDMS-B) reduced roughness in comparison to sample TiO_2-B-10°C, which was found to be insignificant due to physical heterogeneity of the samples. However, coating PDMS on the EPD surface slightly increases the surface roughness from 1 μm to 3 μm ($p < 0.05$). Interestingly, PDMS-B, and PDMS-E show similar static contact angles despite (SCA) having significantly different surface roughness. However, static contact angle measurements of surfaces coated with PDMS (samples PDMS-B, and PDMS-E) revealed contact angles greater 100°, reveling hydrophobic regions regardless of the underlying surface; and the hydrophobic surface

17

with micro-porous structures (PDMS-B) show a much lower roll-off angle than the nano-porous hydrophobic surface (PDMS-E). It was reported that hydrophobic surfaces (high static angles) with nano-scale rough structures may exhibit high roll-off angles (high stick force/high adhesion) associated with air trapped within pores [52, 53] High adhesion results in a greater affinity of bacterial cells to surface and thus sample PDMS-B showing a lower contact angle and low roll off angle indicates for lower affinity.

The engineered surfaces were classified by their hydrophobicities, which are governed by the surface coating (i.e., TiO_2, (P)SiO_2 or PDMS). It was observed that the hydrophobicity was independent of preparation method (BDA, EPD, or spin coating). This was confirmed with TiO_2 (samples TiO_2-B-10°C, TiO_2-B-25°C, TiO_2-BE) layered surfaces, (P)SiO_2 layered surfaces (samples (P)SiO_2-E, (P)SiO_2-BE-25°C, (P)SiO_2-BE-75°C), and PDMS coated samples (PDMS-B, and PDMS-E) ranging in hydrophobicity from superhydrophilic, superhydrophobic and hydrophobic surfaces, respectively. BDA modified surfaces with or without TiO_2 nanoparticle coatings via EPD were found to be superhydrophilic as observed by the static contact angles of zero seen in Table 2. Thus hydraulic diffusivity was measured to identify the degree of hydrophobicity of these samples. This method determined sample TiO_2-BE was less hydrophilic than TiO_2-B-10°C because the nanoparticles coated on the BDA surface make smaller pore sizes and induce higher shear force. Based on the contact angles, samples prepared via EPD of (P)SiO_2 nanoparticles (coated with PDMS) and surfaces coated with PDMS (via spin coating) are classified as hydrophobic surfaces. Surfaces coated with (P)SiO_2 via EPD, are superhydrophobic surfaces with static contact angles greater than 140° (samples

18

(P)SiO2-E, (P)SiO$_2$-BE-25°C, (P)SiO$_2$-BE-75°C). Since the BDA method produces microscale rough-structures on the surface, samples (P)SiO$_2$-BE-25°C and (P)SiO$_2$-BE-75°C, show lower static contact angles than (P)SiO$_2$-E, which has uniform nano-porous structures. It is known that microscale rough-structures are ineffective for enhancing the contact angles [54]. However our results indicate that nano-porous structures creating microscale roughness due indeed affect contact angles.

Quartz surfaces were used for the control surfaces in this work. The surfaces have an average static contact angle of $24 \pm 4°$ but does not show the hydraulic diffusivity because the surfaces are too smooth (the average surface roughness is 1.04 ± 0.18 nm) to generate sufficient capillary pressure. Quartz grains have been shown to have zeta potentials of ~20 mV at 10 mM and ~10 mV at 100 mM [55]. We use these reference zeta-potentials as those of the quartz surfaces when the zeta-potential effects are investigated.

3.3 Bacterial Deposition on Quartz and Engineered Surfaces

Previous studies in the literature have shown that minimal deposition occurs on quartz at lower ionic strength conditions [55-58]. These deposition experiments were designed with the objective of quartz samples to be a comparison point of minimal deposition. Cell deposition on quartz was tested at 10 and 100 mM KCl, resulting in mass transfer rate coefficients of $2.98 \times 10^{-9} \pm 3.88 \times 10^{-10}$ m/s and $1.43 \times 10^{-8} \pm 3.94 \times 10^{-9}$ m/s respectively. Testing quartz below these IS shows deposition to become negligible, in

both parallel plate flow system and column studies [18, 55]. Measured mass transfer rate coefficients of quartz and engineered surfaces are shown in Figure 3a and 3b.

Engineered surfaces modified to produced hydrophilic samples TiO_2-B-10°C, TiO_2-B-25°C, and TiO_2-BE, had mass transfer rate coefficients of $1.25 \times 10^{-8} \pm 8.47 \times 10^{-9}$ m/s, $1.48 \times 10^{-8} \pm 2.86 \times 10^{-9}$ m/s and $1.56 \times 10^{-8} \pm 4.52 \times 10^{-9}$ m/s at 10 mM KCl. Comparison to quartz at 10 mM showed that sample TiO_2-B-10°C was not statistically different ($p > 0.05$) but samples TiO_2-B-25°C, and TiO_2-BE with greater values were found to be statistically different to quartz k_{pp} values ($p<0.05$). At 100 mM KCl, the mass transfer rates coefficients where $1.60 \times 10^{-8} \pm 3.12 \times 10^{-10}$ m/s, $2.26 \times 10^{-8} \pm 5.68 \times 10^{-9}$ m/s and $2.06 \times 10^{-8} \pm 1.43 \times 10^{-9}$ m/s for samples TiO_2-B-10°C, TiO_2-B-25°C, and TiO_2-BE samples. At this IS, samples TiO_2-B-10°C and TiO_2-B-25°C were not statistically different from quartz k_{pp} values ($p > 0.05$), but TiO_2-BE did show a statistical difference with greater k_{pp} values compared to k_{pp} quartz ($p < 0.05$), indicating that these surfaces will promote microbial attachment in comparison to the quartz samples.

The engineered surfaces prepared via deposition of PDMS coated SiO_2 ((P)SiO_2-E, (P)SiO_2-BE-25°C, and (P)SiO_2-BE-75°C) were found to be superhydrophobic and had k_{pp} values of $6.94 \times 10^{-9} \pm 3.26 \times 10^{-9}$ m/s, $7.14 \times 10^{-9} \pm 6.16 \times 10^{-10}$ m/s and $5.56 \times 10^{-8} \pm 3.75 \times 10^{-9}$ m/s at 10 mM KCl, respectively. Samples (P)SiO_2-E and (P)SiO_2-BE-25°C were found to be statistically different to quartz, having larger k_{pp} values ($p < 0.05$). (P)SiO_2-BE-75°C was found to have statistically insignificant deposition as with quartz ($p > 0.5$) at 10 mM KCl.
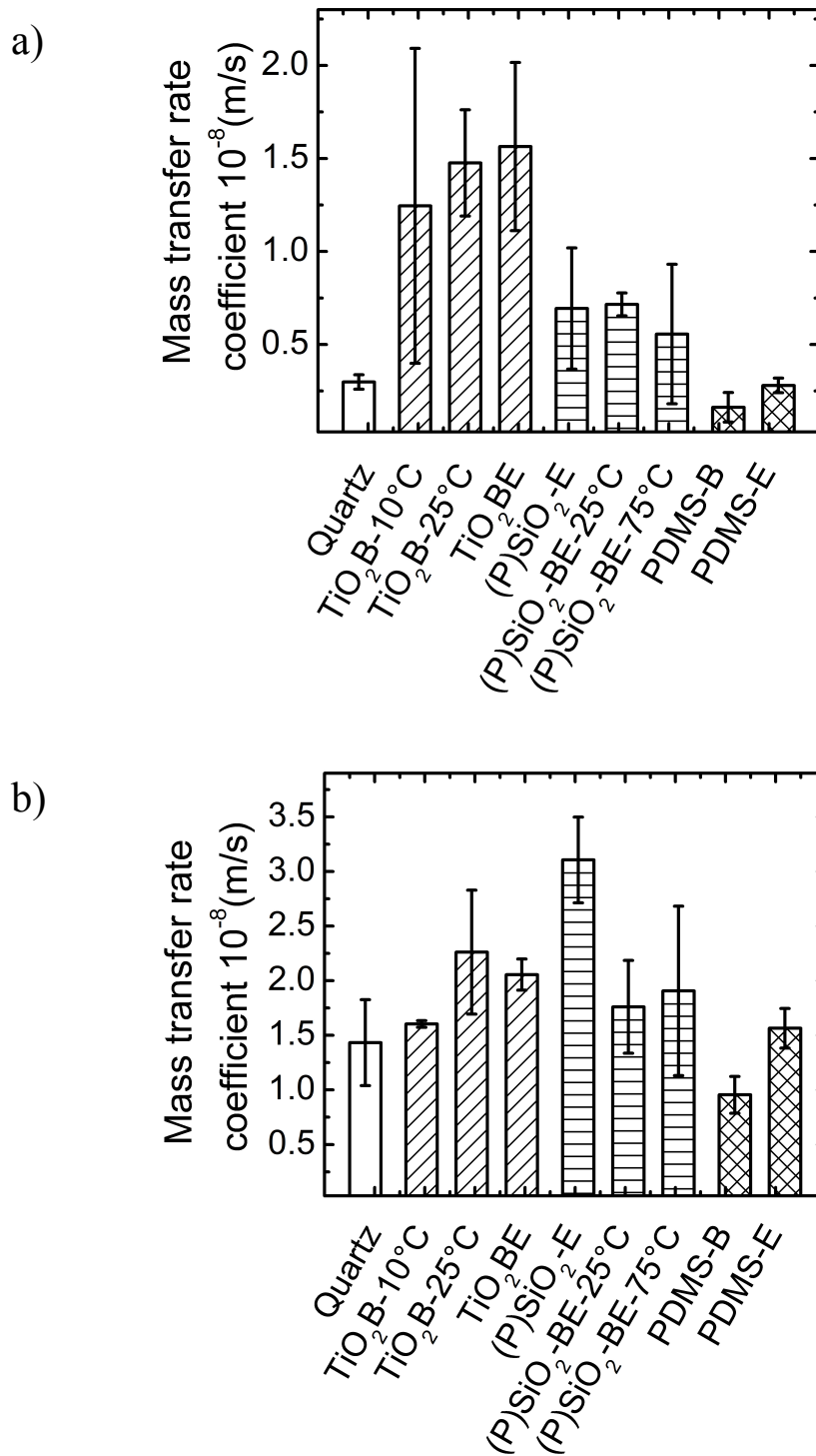
a)

b)

Figure 3. Mass transfer rates, k_{pp}, of *H. pacifica g* onto quartz and novel surfaces in the parallel plate flow chamber systems at the ionic strength of (a) 10 mM KCl and (b) 100 mM KCl. Experiments carried out at temperature (22-25 °C) and ambient pH (5.6-5.8). Error bars indicate standard deviation.

Similar to what was observed for the TiO_2-based samples, there was an increase in mass transfer rate coefficients at the elevated ionic strength of 100 mM KCl (to $3.11\times10^{-8} \pm 3.29\times10^{-9}$ m/s, $1.76\times10^{-8} \pm 4.24\times10^{-9}$ m/s and $1.91\times10^{-8} \pm 7.76\times10^{-9}$ m/s for (P)SiO_2-E, (P)SiO_2-BE-25°C, and (P)SiO_2-BE-75°C, respectively). At 100 mM KCl, (P)SiO_2-E sample was found to be statistically different then quartz due to great k_{pp} values (p < 0.05) but (P)SiO_2-BE-25°C, and (P)SiO_2-BE-75°C were not found to statistically different (p > 0.05). Thus there was no clear trend distinguishing the superhydrophobic coatings and clean quartz.

The PDMS coated surfaces (PDMS-B and PDMS-E), resulted in surfaces that were hydrophobic and showed mass transfer rates coefficients of $1.68\times10^{-9} \pm 8.71\times10^{-10}$ m/s and $2.80\times10^{-9} \pm 3.92\times10^{-10}$ m/s at 10 mM KCl, respectively. The k_{pp} value of PDMS-B is significantly less than quartz at 10 mM (p > 0.05). Values at 100 mM which were found to be $9.55\times10^{-9} \pm 1.68\times10^{-9}$ m/s and $1.56\times10^{-9} \pm 1.82\times10^{-9}$ m/s. In comparison to quartz at 100 mM, PDMS-B showed the less cell attachment rate with a statistical difference of p > 0.05. The treatment with PDMS on micro-porous surfaces produced by BDA resulted in deposition less than that of quartz, effectively indicating that BDA and EPD surface overlaid with poly(dimethyl siloxane) (PDMS) appeared to be most resistant to cell attachment.

3.4 Mechanisms of Attachment

Greater deposition rates were observed under higher ionic strength. The intensity of electrostatic repulsion between Figure 3a and 3b shows sensitivity to the IS of the

solution [59]. Increased IS resulted in a decrease in electrostatic repulsive forces, leading to increased bacterial cell attachment as noted in Figures 3a and 3b. All samples showed sensitivity for IS therefore electrostatic interactions significantly governed cell deposition.

Test surfaces TiO_2-B-10°C, TiO_2-B-25°C, TiO_2-BE had the greatest deposition of cells as anticipated due to their superhydrophilic nature, which interacted favorably with the highly hydrophilic cells of *H. pacifica* g. Engineered superhydrophobic surfaces (P)SiO_2-E, (P)SiO_2-BE-25°C, and (P)SiO_2-BE-75°C were expected to have the least amount of bacterial cells deposit; however, they showed greater deposition then that of the hydrophobic surfaces (PDMS-B and PDMS-E). Test surfaces PDMS-B, and PDMS-E showed deposition of cells to be similar to or less than quartz samples; There is potential for future applications of PDMS as the primary strategy to achieve an antifouling surface, which has been corroborated by other studies[60]

Mass transfer rates of cells onto the hydrophilic surfaces (TiO_2-B-10°C, TiO_2-B-25°C, and TiO_2-BE) and quartz as are shown in Figure 4a as function of roughness. There is a correlation with increased roughness as k_{pp} values are increased. In Figure 4b there is further indication that hydrophilicity was dependent on roughness; therefore these samples are sensitive to roughness only. This is supported by a previous study reporting roughness attributes to overall attachment, and thus promoting bacterial adhesion [61].

The mass transfer rate coefficients of the *H. pacifica* g on hydrophobic samples (P)SiO_2-E, (P)SiO_2-BE-25°C, (P)SiO_2-BE-75°C, PDMS-B, and PDMS-E in comparison to roughness are shown in Figure 5a.

a)

b)
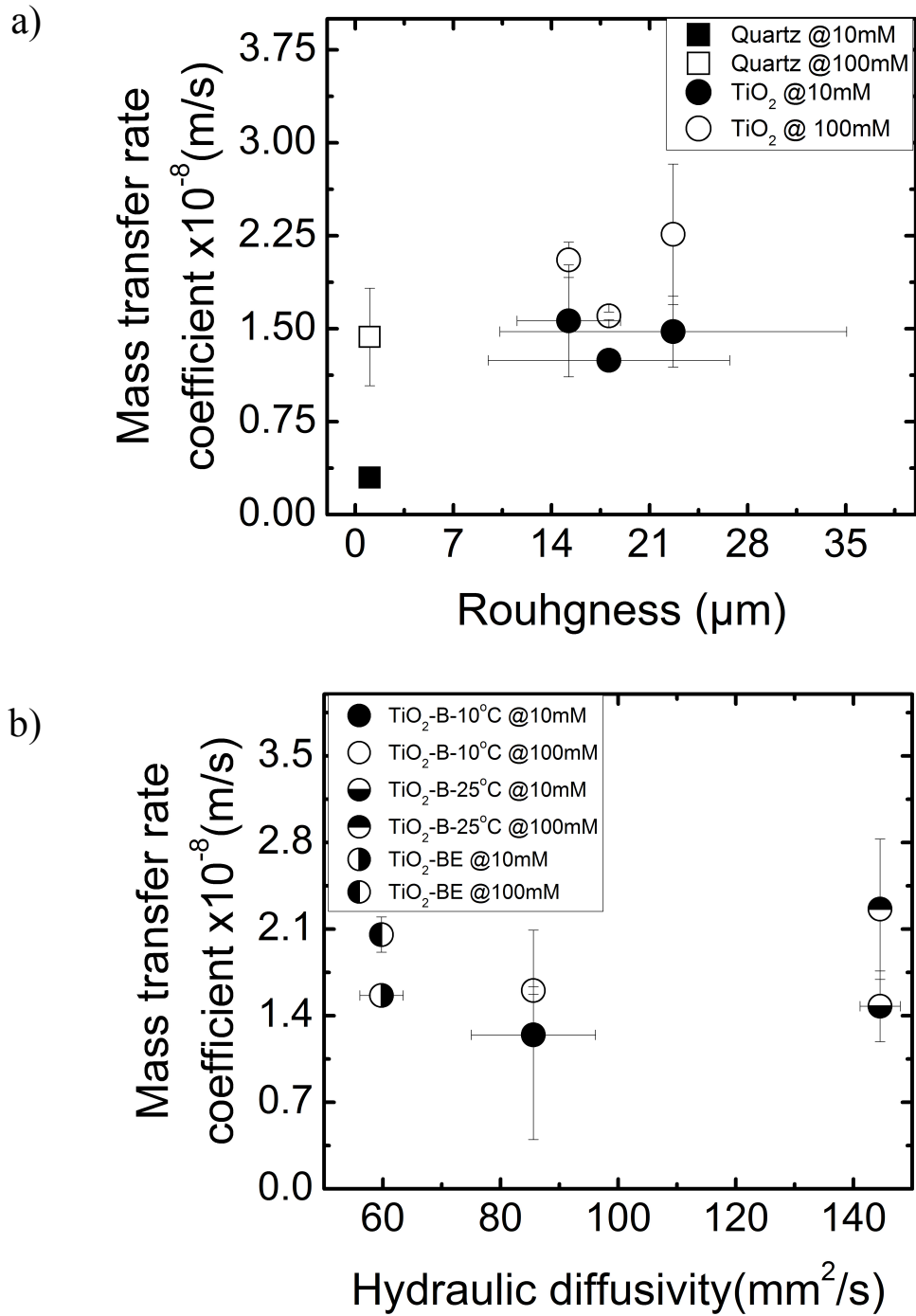
Figure 4. Mass transfer rates, k_{pp}, of *H. pacifica g* compared to (a) roughness at both 10 mM KCl and 100 mM KCl and indicating a slight increase in k_{pp} values with increase in roughness (b) hydraulic diffusivity and indicates hydrophilicity is not a factor in k_{pp} value.

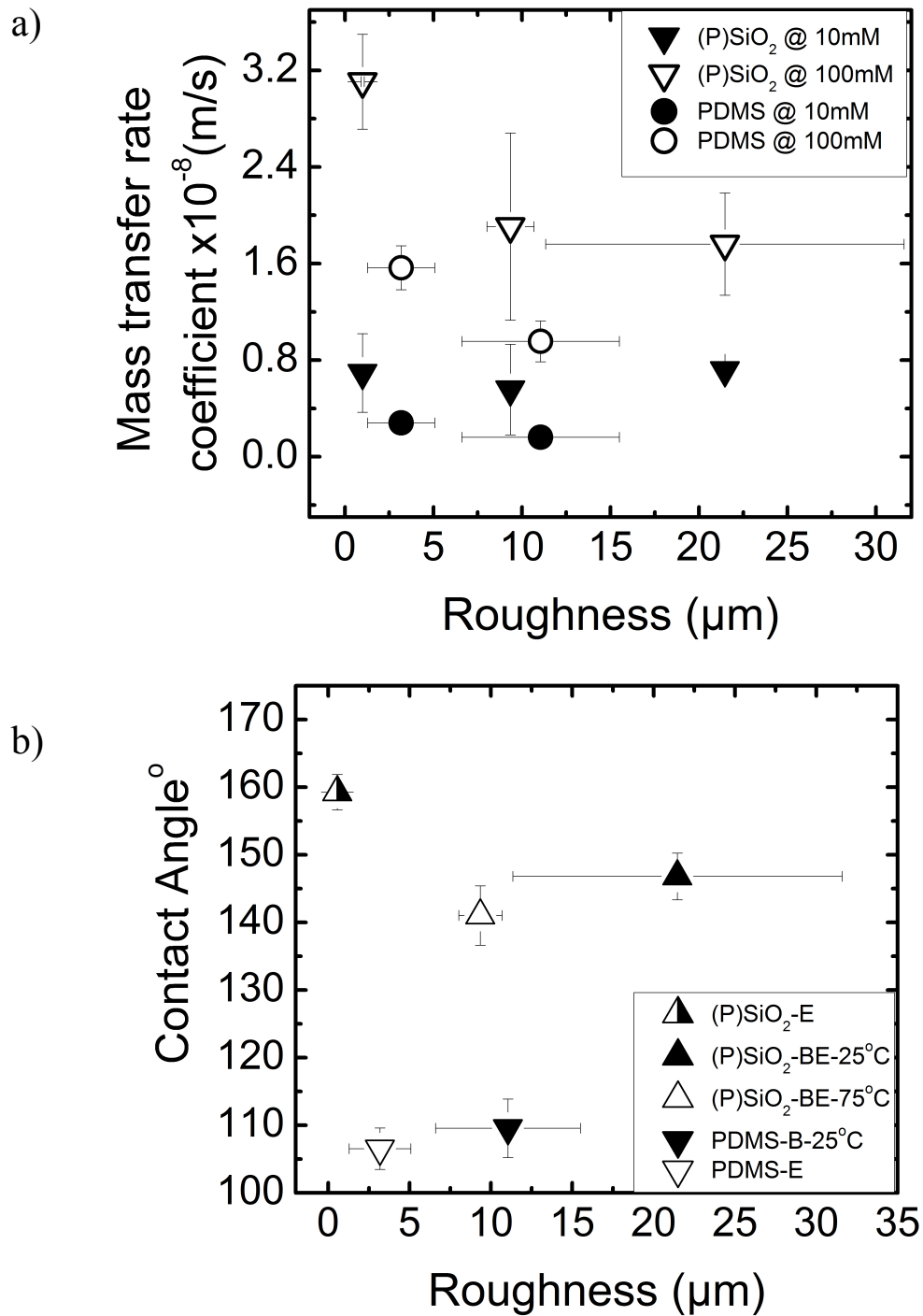**Figure 5.** Roughness of surfaces covered in PDMS in comparison to (a) mass transfer rates, k_{pp}, of *H. pacifica g* at 10 mM KCl and 100 mM KCl showing a slight decrease with increase of roughness but not definitive (b) contact angle values indicating a slight effect of roughness for a majority of sample.

There may be a correlation with roughness and k_{pp} values; however, we were

unable to quantify this due to the limited sampling. The trend suggests (Figure 5a) that

the k_{pp} values slightly decrease with increase roughness but it is uncertain if the trend

plateausplenteous or may continue to increase. Therefore, there is opportunity to optimize

roughness such that we canreduce microbial adhesion. There is a more apparent impact at

the higher IS condition (100 mM) as seen in Figure 5a, which is comparable to more

brackish waters indicating that surface roughness may be exploited in such systems for

controlling cell attachment. There is also a correlation between contact angle and

roughness in hydrophobic surfaces as shown in Figure 5b, which indicates a slight

increase in contact angle as roughness is increased for comparable samples.

3.5 Conclusion

We have investigated cell attachment via the mass transfer coefficients on

different engineered surfaces produced by EPD, BDA, and spin coating with PDMS. The

resulting surfaces showed hydrophobicity ranges from superhydrophilic to

superhydrophobic with different rough scales and nano-porous and micro-porous

structures produced by EPD of nanoparticles and BDA with PDMS spin coating,

respectively. The effects of the different roughness scales were reflected especially by the

roll-off angles on hydrophobic surfaces, showing low roll-off angles on micro-scale

rough surfaces.

"Anti-fouling" surfaces, as defined as surfaces with mass transfer rates similar to

quartz surfaces, were successfully produced by BDA and spin coating with PDMS

(sample PDMS-B). From the SEM images and the surface roughness data, the surfaces are composed of micron scale bumps and relatively large surface roughness. The surface characteristics were indicated by hydrophobic surfaces with 110° static contact angles and of 5° roll-off angles, attributed by PDMS and the micro-scale rough structures.

The engineered surfaces, which were superhydrophilic, displayed higher mass transfer rates than the hydrophobic and superhydrophobic surfaces. This observation was due to the favorable interaction found between the hydrophilic bacterial cells with superhydrophilic surfaces. The difference of mass transfer rates between the hydrophobic surfaces decreased with greater ionic strength because the electrostatic interactions overwhelmed other interaction forces.

The incorporation PDMS coated SiO_2 and TiO_2 nanoparticles increased mass transfer to the surface as compared to pure BD techniques for each engineered surface. For example, TiO_2-BE, SiO_2-E, and PDMS-E showed greater mass transfer rates than TiO_2B-10°C and -25°C, SiO_2-BE-25°C and -75°C, and PDMS-B, respectively. Thus indicating that the presence of nanoscale structures created sufficient roughness as to enhance cell-attachment.

The engineered hydrophobic surface PDMS-B showed lower mass transfer rates than PDMS-E even though static contact angle data showed no difference between two surfaces. This was due to PDMS-B having more micro structures, which can be verified from roll-off angles and also roughness data. PDMS-B revealed much lower roll-off angles than PDMS-E indicating that PDMS-B has less nano scale rough structures than

PDMS-E. It is well known that nano structures enhance contact angle hysteresis, resulting in high roll-off angle [52].

Results indicate that TiO_2-BE presented the greatest mass transfer rates because it is superhydrophilic and has nano structures attributed to the TiO_2 nanoparticles deposited by EPD on the micro-porous structures produced by BDA. However, PDMS-B showed the best "anti-fouling" performance due to its hydrophobicity and micro-porous structures. Therefore, in the case of hydrophilic bacteria, we can expect that surfaces that are hydrophobic and have low roll-off angles will be the best candidates for anti-fouling performance. In contrast, superhydrophilic surfaces that have nano rough structures will likely induce biofouling.

These novel engineered surfaces show properties that can be functional to a variety of industries. Engineered surfaces produced by breakdown anodization that were spin coated with PDMS (sample PDMS-B) have the potential for applications on various marine surfaces (i.e. ship hulls). These surfaces showed similar results to our control samples (quartz) and may be the most durable of the engineered surfaces. The ionic strengths tested indicate that these PDMS coated surfaces would be best for fresh water or brackish systems. This work has demonstrated that through these engineering approaches, we have the ability to alter surfaces at the nano- and micro- scale by a combination of techniques. This gives potential for manipulation and thus allowing for fine-tuning the properties of the materials for the particular aquatic environment in question.

References

[1]   H. C. Flemming, A. Tamachkiarowa, J. Klahre, and J. Schmitt, "Monitoring of fouling and biofouling in technical systems," *Water Science and Technology,* vol. 38, pp. 291-298, 1998.

[2]   R. L. Townsin, "The Ship Hull Fouling Penalty," *Biofouling,* vol. 19, pp. 9-15, 2003.

[3]   P. K. Abdul Azis, I. Al-Tisan, and N. Sasikumar, "Biofouling potential and environmental factors of seawater at a desalination plant intake," *Desalination,* vol. 135, pp. 69-82, 2001.

[4]   M. P. Schultz, J. A. Bendick, E. R. Holm, and W. M. Hertel, "Economic impact of biofouling on a naval surface ship," *Biofouling,* vol. 27, pp. 87-98, 2010.

[5]   M. E. Callow and J. A. Callow, "Marine biofouling: a sticky problem," *Biologist,* vol. 49, pp. 1-5, 2002.

[6]   H. C. Flemming, "Why Microorganisms Live in Biofilms and the Problem of Biofouling," in *Marine and Industrial Biofouling*. vol. 4, H.-C. Flemming, P. S. Murthy, R. Venkatesan, and K. Cooksey, Eds., ed: Springer Berlin Heidelberg, 2009, pp. 3-12.

[7]   K. A. Dafforn, J. A. Lewis, and E. L. Johnston, "Antifouling strategies: history and regulation, ecological impacts and mitigation," *Marine Pollution Bulletin,* vol. 62, pp. 453-465, 2011.

[8]   G. Borkow and J. Gabbay, "Copper as a biocidal tool," *Current medicinal chemistry,* vol. 12, pp. 2163-2175, 2005.

[9]   A. P. Negri and A. J. Heyward, "Inhibition of coral fertilisation and larval metamorphosis by tributyltin and copper," *Marine Environmental Research,* vol. 51, pp. 17-27, 2001.

[10]   M. A. Champ, "Economic and environmental impacts on ports and harbors from the convention to ban harmful marine anti-fouling systems," *Marine Pollution Bulletin,* vol. 46, pp. 935-940, 2003.

[11]   R. T. Carson, M. Damon, L. T. Johnson, and J. A. Gonzalez, "Conceptual issues in designing a policy to phase out metal-based antifouling paints on recreational boats in San Diego Bay," *Journal of Environmental Management,* vol. 90, pp. 2460-2468, 2009.

[12]   N. Singhasemanon, "U.S. Environmental Protection Agency Registration Review for Coppers," M. A. A. Coordinator, Ed., ed. Washington, Distric of Columbia: Department of Pesticide Regulation, December 16, 2010, p. 12.

[13]   S. Schulte, J. Wingender, and H. C. Flemming, "Efficacy of biocides against biofilms," in *Directory of Microbicides for the Protection of Materials*, W. Paulus, Ed., ed: Springer Netherlands, 2005, pp. 93-120.

[14]   T. R. Thatiparti, A. J. Shoffstall, and H. A. von Recum, "Cyclodextrin-based device coatings for affinity-based release of antibiotics," *Biomaterials,* vol. 31, pp. 2335-2347, 2010.

[15] D. Coleman, M. O'Donnell, A. Shore, and R. Russell, "Biofilm problems in dental unit water systems and its practical control," *Journal of applied microbiology,* vol. 106, pp. 1424-1437, 2009.

[16] E. Ralston and G. Swain, "Bioinspiration—the solution for biofouling control?," *Bioinspiration & biomimetics,* vol. 4, pp. 1-9, 2009.

[17] M. E. Callow, J. A. Callow, L. K. Ista, S. E. Coleman, A. C. Nolasco, and G. P. López, "Use of Self-Assembled Monolayers of Different Wettabilities To Study Surface Selection and Primary Adhesion Processes of Green Algal (Enteromorpha) Zoospores," *Applied and Environmental Microbiology,* vol. 66, pp. 3249-3254, 2000.

[18] G. Chen, D. E. Beving, R. S. Bedi, Y. S. Yan, and S. L. Walker, "Initial Bacterial Deposition on Bare and Zeolite-Coated Aluminum Alloy and Stainless Steel," *Langmuir,* vol. 25, pp. 1620-1626, 2009.

[19] C. M. Grozea and G. C. Walker, "Approaches in designing non-toxic polymer surfaces to deter marine biofouling," *Soft Matter,* vol. 5, pp. 4088-4100, 2009.

[20] S. Krishnan, N. Wang, C. K. Ober, J. A. Finlay, M. E. Callow, J. A. Callow, A. Hexemer, K. E. Sohn, E. J. Kramer, and D. A. Fischer, "Comparison of the Fouling Release Properties of Hydrophobic Fluorinated and Hydrophilic PEGylated Block Copolymer Surfaces: Attachment Strength of the Diatom Navicula and the Green Alga Ulva," *Biomacromolecules,* vol. 7, pp. 1449-1462, 2006.

[21] J. C. Love, L. A. Estroff, J. K. Kriebel, R. G. Nuzzo, and G. M. Whitesides, "Self-assembled monolayers of thiolates on metals as a form of nanotechnology," *Chemical reviews,* vol. 105, pp. 1103-1170, 2005.

[22] S. Sommer, A. Ekin, D. C. Webster, S. J. Stafslien, J. Daniels, L. J. VanderWal, S. E. Thompson, M. E. Callow, and J. A. Callow, "A preliminary study on the properties and fouling-release performance of siloxane–polyurethane coatings prepared from poly (dimethylsiloxane)(PDMS) macromers," *Biofouling,* vol. 26, pp. 961-972, 2010.

[23] P. Thebault, E. T. d. Givenchy, S. Géribaldi, R. Levy, Y. Vandenberghe, and F. Guittard, "Surface and antimicrobial properties of semi-fluorinated quaternary ammonium thiol surfactants potentially usable for Self-Assembled Monolayers," *Journal of Fluorine Chemistry,* vol. 131, pp. 592-596, 2010.

[24] A. Ulman, "Formation and structure of self-assembled monolayers," *Chemical reviews,* vol. 96, pp. 1533-1554, 1996.

[25] D. L. Schmidt, R. F. Brady, K. Lam, D. C. Schmidt, and M. K. Chaudhury, "Contact Angle Hysteresis, Adhesion, and Marine Biofouling," *Langmuir,* vol. 20, pp. 2830-2836, 2004.

[26] T. R. Scheuerman, A. K. Camper, and M. A. Hamilton, "Effects of Substratum Topography on Bacterial Adhesion," *Journal of Colloid and Interface Science,* vol. 208, pp. 23-33, 1998.

[27]   N. Mitik Dineva, J. Wang, R. C. Mocanasu, P. R. Stoddart, R. J. Crawford, and E. P. Ivanova, "Impact of nano topography on bacterial attachment," *Biotechnology journal,* vol. 3, pp. 536-544, 2008.

[28]   R. F. Brady and I. L. Singer, "Mechanical factors favoring release from fouling release coatings," *Biofouling,* vol. 15, pp. 73-81, 2000.

[29]   S. L. Hodson, C. M. Burke, and A. P. Bissett, "Biofouling of fish-cage netting: the efficacy of a silicone coating and the effect of netting colour," *Aquaculture,* vol. 184, pp. 277-290, 2000.

[30]   G. Swain, S. Herpe, E. Ralston, and M. Tribou, "Short-term testing of antifouling surfaces: the importance of colour," *Biofouling,* vol. 22, pp. 425-429, 2006.

[31]   S. Dobretsov, R. M. Abed, and C. R. Voolstra, "The effect of surface colour on the formation of marine micro and macrofouling communities," *Biofouling,* pp. 1-11, 2013.

[32]   Y. S. Joung and C. R. Buie, "A Hybrid Method Employing Breakdown Anodization and Electrophoretic Deposition for Superhydrophilic Surfaces," *The Journal of Physical Chemistry B,* vol. 117, pp. 1714-1723, 2013.

[33]   Y. S. Joung and C. R. Buie, "Electrophoretic Deposition of Unstable Colloidal Suspensions for Superhydrophobic Surfaces," *Langmuir,* vol. 27, pp. 4156-4163, 2011.

[34]   D. P. Bakker, F. M. Huijs, J. de Vries, J. W. Klijnstra, H. J. Busscher, and H. C. van der Mei, "Bacterial deposition to fluoridated and non-fluoridated polyurethane coatings with different elastic modulus and surface tension in a parallel plate and a stagnation point flow chamber," *Colloids and Surfaces B: Biointerfaces,* vol. 32, pp. 179-190, 2003.

[35]   G. Chen and S. L. Walker, "Role of Solution Chemistry and Ion Valence on the Adhesion Kinetics of Groundwater and Marine Bacteria," *Langmuir,* vol. 23, pp. 7162-7169, 2007.

[36]   S. J. Dobson and P. D. Franzmann, "Unification of the Genera Deleya (Baumann et al. 1983), Halomonas (Vreeland et al. 1980), and Halovibrio (Fendrich 1988) and the Species Paracoccus halodenitrificans (Robinson and Gibbons 1952) into a Single Genus, Halomonas, and Placement of the Genus Zymobacter in the Family Halomonadaceae," *International Journal of Systematic Bacteriology,* vol. 46, pp. 550-558, 1996.

[37]   D. P. Bakker, H. J. Busscher, and H. C. van der Mei, "Bacterial deposition in a parallel plate and a stagnation point flow chamber: microbial adhesion mechanisms depend on the mass transport conditions," *Microbiology,* vol. 148, pp. 597-603, 2002.

[38]   M. Rosenberg, D. Gutnick, and E. Rosenberg, "Adherence of bacteria to hydrocarbons: A simple method for measuring cell-surface hydrophobicity," *FEMS Microbiology Letters,* vol. 9, pp. 29-33, 1980.

[39]   R. S. Pembrey, K. C. Marshall, and R. P. Schneider, "Cell Surface Analysis Techniques: What Do Cell Preparation Protocols Do to Cell Surface

Properties?," *Applied and Environmental Microbiology,* vol. 65, pp. 2877-2894, 1999.

[40] M. A. Ali and D. A. Dzombak, "Effects of simple organic acids on sorption of Cu2+ and Ca2+ on goethite," *Geochimica et Cosmochimica Acta,* vol. 60, pp. 291-304, 1996.

[41] M. Elimelech, X. Jia, J. Gregory, and R. Williams, *Particle deposition & aggregation: measurement, modelling and simulation*: Butterworth-Heinemann, 1998.

[42] H. N. Kim, S. A. Bradford, and S. L. Walker, "Escherichia coli O157:H7 Transport in Saturated Porous Media: Role of Solution Chemistry and Surface Macromolecules," *Environmental Science & Technology,* vol. 43, pp. 4340-4347, 2009.

[43] Y. S. Joung and C. R. Buie, "Hybrid Electrophoretic Deposition with Anodization Process for Superhydrophilic Surfaces to Enhance Critical Heat Flux," *Key Engineering Materials,* vol. 507, 2012.

[44] K. H. Chu, Y. S. Joung, R. Enright, C. R. Buie, and E. N. Wang, "Hierarchically Structured Surfaces for Boiling Critical Heat Flux Enhancement," *Applied Physics Letters,* vol. 102, pp. 151602-4, 2013.

[45] D. Oner and T. J. McCarthy, "Ultrahydrophobic surfaces. Effects of topography length scales on wettability," *Langmuir,* vol. 16, pp. 7777-7782, 2000.

[46] A. Siebold, A. Walliser, M. Nardin, M. Oppliger, and J. Schultz, "Capillary Rise for Thermodynamic Characterization of Solid Particle Surface," *Journal of Colloid and Interface Science,* vol. 186, pp. 60-70, 1997.

[47] S. L. Walker, S. Bhattacharjee, E. M. V. Hoek, and M. Elimelech, "A Novel Asymmetric Clamping Cell for Measuring Streaming Potential of Flat Surfaces," *Langmuir,* vol. 18, pp. 2193-2198, 2002.

[48] J. T. Patton, D. G. Mentor, D. M. Benson, G. L. Nicolson, and L. V. McIntire, "Computerized analysis of tumor cells flowing in a parallel plate chamber to determine their adhesion stabilization lag time," *Cell Motility and the Cytoskeleton,* vol. 26, pp. 88-98, 1993.

[49] T. R. Kline, G. Chen, and S. L. Walker, "Colloidal Deposition on Remotely Controlled Charged Micropatterned Surfaces in a Parallel-Plate Flow Chamber," *Langmuir,* vol. 24, pp. 9381-9385, 2008.

[50] Z. Adamczyk and T. G. M. Van De Ven, "Deposition of particles under external forces in laminar flow through parallel-plate and cylindrical channels," *Journal of Colloid and Interface Science,* vol. 80, pp. 340-356, 1981.

[51] I. Chowdhury and S. L. Walker, "Deposition mechanisms of TiO2 nanoparticles in a parallel plate system," *Journal of Colloid and Interface Science,* vol. 369, pp. 16-22, 2012.

[52] B. Balu, V. Breedveld, and D. W. Hess, "Fabrication of "Roll-off" and "Sticky" Superhydrophobic Cellulose Surfaces via Plasma Processing," *Langmuir,* vol. 24, pp. 4785-4790, 2008.

[53]   E. Bormashenko, R. Pogreb, G. Whyman, and A. Musin, "Surface tension of liquid marbles," *Colloids and Surfaces A: Physicochemical and Engineering Aspects,* vol. 351, pp. 78-82, 2009.

[54]   Y. W. Lee, S. H. Park, K. B. Kim, and J. K. Lee, "Fabrication of hierarchical structures on a polymer surface to mimic natural superhydrophobic surfaces," *Advanced Materials,* vol. 19, p. 2330, Sep 2007.

[55]   J. A. Redman, S. L. Walker, and M. Elimelech, "Bacterial adhesion and transport in porous media: Role of the secondary energy minimum," *Environmental Science & Technology,* vol. 38, pp. 1777-1785, 2004.

[56]   A. L. Mills, J. S. Herman, G. M. Hornberger, and T. H. DeJesús, "Effect of Solution Ionic Strength and Iron Coatings on Mineral Grains on the Sorption of Bacterial Cells to Quartz Sand," *Applied and Environmental Microbiology,* vol. 60, pp. 3300-3306, 1994.

[57]   N.-C. Choi, D.-J. Kim, and S.-B. Kim, "Quantification of bacterial mass recovery as a function of pore-water velocity and ionic strength," *Research in Microbiology,* vol. 158, pp. 70-78, 2007.

[58]   W. P. Johnson, M. J. Martin, M. J. Gross, and B. E. Logan, "Facilitation of bacterial transport through porous media by changes in solution and surface properties," *Colloids and Surfaces A: Physicochemical and Engineering Aspects,* vol. 107, pp. 263-271, 1996.

[59]   H. H. M. Rijnaarts, W. Norde, J. Lyklema, and A. J. B. Zehnder, "DLVO and steric contributions to bacterial deposition in media of different ionic strengths," *Colloids and Surfaces B: Biointerfaces,* vol. 14, pp. 179-195, 1999.

[60]   M. Lejars, A. Margaillan, and C. Bressy, "Fouling Release Coatings: A Nontoxic Alternative to Biocidal Antifouling Coatings," *Chemical reviews,* vol. 112, pp. 4347-4390, 2012/08/08 2012.

[61]   H. Tang, T. Cao, X. Liang, A. Wang, S. O. Salley, J. McAllister, and K. Y. Ng, "Influence of silicone surface roughness and hydrophobicity on adhesion and colonization of Staphylococcus epidermidis," *Journal of biomedical materials research. Part A,* vol. 88, pp. 454-463, 2009.